THE JOURNAL OF BIOLOGICAL CHEMISTRY

Vol. 276, No. 24, Issue of June 15, pp. 21951–21959, 2001
Printed in U.S.A.

The *Ataxia telangiectasia* Gene Product Is Required for Oxidative Stress-induced G_1 and G_2 Checkpoint Function in Human Fibroblasts*

Received for publication, December 14, 2000, and in revised form, March 19, 2001
Published, JBC Papers in Press, April 4, 2001, DOI 10.1074/jbc.M011303200

Rodney E. Shackelford, Cynthia L. Innes, Stella O. Sieber, Alexandra N. Heinloth, Steven A. Leadon‡, and Richard S. Paules§

From the Growth Control and Cancer Group, NIEHS, National Institutes of Health, Research Triangle Park, North Carolina 27709 and the ‡Department of Radiation Oncology, University of North Carolina School of Medicine, Chapel Hill, North Carolina 27599

Ataxia telangiectasia (AT) is an autosomal recessive disorder characterized by neuronal degeneration accompanied by ataxia, telangiectasias, acute cancer predisposition, and sensitivity to ionizing radiation (IR). Cells from individuals with AT show unusual sensitivity to IR, severely attenuated cell cycle checkpoint functions, and poor p53 induction in response to IR compared with normal human fibroblasts (NHFs). The gene mutated in AT (*ATM*) has been cloned, and its product, pATM, has IR-inducible kinase activity. The AT phenotype has been suggested to be a consequence, at least in part, of an inability to respond appropriately to oxidative damage. To test this hypothesis, we examined the ability of NHFs and AT dermal fibroblasts to respond to *t*-butyl hydroperoxide and IR treatment. AT fibroblasts exhibit, in comparison to NHFs, increased sensitivity to the toxicity of *t*-butyl hydroperoxide, as measured by colony-forming efficiency assays. Unlike NHFs, AT fibroblasts fail to show G_1 and G_2 phase checkpoint functions or to induce p53 in response to *t*-butyl hydroperoxide. Treatment of NHFs with *t*-butyl hydroperoxide activates pATM-associated kinase activity. Our results indicate that pATM is involved in responding to certain aspects of oxidative damage and in signaling this information to downstream effectors of the cell cycle checkpoint functions. Our data further suggest that some of the pathologies seen in AT could arise as a consequence of an inability to respond normally to oxidative damage.

Ataxia telangiectasia (AT)[1] is an autosomal recessive disorder characterized by immune disorders, acute cancer predisposition, telangiectasias, sensitivity to ionizing radiation (IR), and neuronal degeneration (1). The number of individuals who carry one defective copy of the AT gene has been estimated to be around 0.5–1% of the general population (2). Those AT heterozygotes have been reported to exhibit elevated cancer risk, particularly for breast cancer and lymphoproliferative disease (3–5). Cultured AT dermal fibroblasts show increased chromosomal instability and acute sensitivity to IR in comparison to age-matched normal human fibroblasts (NHFs) (6–10). Cells from individuals with AT exhibit poor p53 induction and severely impaired G_1, S, and G_2 phase checkpoint functions in response to IR (11–14). The gene mutated in AT, *ATM*, has been identified (15), and the gene product, pATM, has been shown to have IR-inducible protein kinase activity (16, 17). *ATM* shares homology with the family of phosphatidylinositol 3′-kinases (15), which include DNA-PK, ATR, MEC1, TEL1, TOR, and FRAP among others (18). Members of this family of proteins have been reported to be involved in various aspects of the detection of DNA damage and control of cell cycle progression (18, 19).

pATM has been suggested to function, at least in part, in the cellular response to oxidative damage (for review see Ref. 20). Support for this hypothesis comes from observations that pATM-deficient cells are unusually sensitive to the toxic effects of hydrogen peroxide, nitric oxide, and superoxide treatment as determined by colony-forming efficiency assays. Additionally, they resynthesize glutathione unusually slowly after depletion with diethyl maleate (21–25). Furthermore, Barlow and colleagues (26) have shown that *ATM*-deficient mice have elevated markers of oxidative stress, particularly in organs such as the cerebellum, which are consistently affected in individuals with AT. Therefore, we hypothesized that pATM-deficient fibroblasts would lack normal cell cycle checkpoint function in response to oxidative stress. To test this hypothesis, we compared the effect of IR, and reactive oxygen species produced by treatment with *t*-butyl hydroperoxide, on normal and *ATM*-deficient human fibroblast strains.

EXPERIMENTAL PROCEDURES

Cell Cultures and Culture Conditions—NHF1 is a normal human fibroblast culture derived from foreskins of apparently healthy neonates and was used at passages 13–19 (27). GM03349, a normal dermal fibroblast strain from a 10-year-old male, was obtained from NIGMS (National Institutes of Health) Human Genetic Mutant Cell Repository (Camden, NJ) and used at passages 15–19. *ATM*-deficient dermal fibroblasts were obtained from the NIGMS Human Genetic Mutant Cell Repository (strain designations GM02052 and GM03395 (Camden, NJ)) and the NIA Aging Cell Repository (strain AG03058 (Camden, NJ)). The donor for the cells of strain GM02052 was a 15-year-old Moroccan female. Cells of this strain contain a mutation at nucleotide 103 that causes a change in coding from cysteine to thymidine, resulting in a stop codon at position 35 (28). The cells of strain GM03395 are dermal fibroblasts cultured from a skin biopsy of a 13-year-old black male, and

* This work was supported in part by United States Public Health Service Grant CA40453 (to S. A. L.). The costs of publication of this article were defrayed in part by the payment of page charges. This article must therefore be hereby marked "*advertisement*" in accordance with 18 U.S.C. Section 1734 solely to indicate this fact.

§ To whom correspondence should be addressed: Growth Control and Cancer Group, NIEHS, National Institutes of Health, Mail Drop F1-05, 111 Alexander Dr., P. O. Box 12233, Research Triangle Park, NC 27709. Tel.: 919-541-3710; Fax: 919-541-1460; E-mail: paules@niehs.nih.gov.

[1] The abbreviations used are: AT, ataxia telangiectasia; αATM 7 a.p., affinity-purified αATM 7 antibody; pATM, ataxia telangiectasia-mutated gene product; BrdUrd, 5-bromo-2′-deoxyuridine; BSA, bovine serum albumin; DAPI, 4′,6-diamidino-2-phenylindole; HO-1, heme oxygenase-1; IR, ionizing radiation; NHF, normal human fibroblast; PBS, phosphate buffered saline; Gy, gray; PBS, phosphate-buffered saline; PAGE, polyacrylamide gel electrophoresis.

the cells of strain AG03058 are dermal fibroblasts cultured from a skin biopsy from a 14-year-old black female. The exact mutations of *ATM* in strains GM03395 and AG03058 are not known. However, no pATM could be detected by immunoblotting in protein extracts from any of these strains, and the donors expressed the typical phenotype of the AT disease. These cells were used at passages 14–20. Normal human fibroblasts (NHF1 and GM03349 strains) were grown at 37 °C in a humidified 5% CO_2 atmosphere in minimum Eagle's medium, supplemented with 10% fetal bovine serum (Life Technologies, Inc.) and 2 mM glutamine (Life Technologies, Inc.) (NHF medium). *ATM*-deficient fibroblasts (GM02052, GM03395, and AG03058) were grown under the same conditions in minimum Eagle's medium supplemented with 20% fetal bovine serum, 2 mM glutamine, 0.4 mM serine, 0.2 mM aspartic acid, and 2 mM pyruvic acid (AT medium) (14). HeLa cells, obtained from the American Type Culture Collection (Manassas, VA), were cultured as above in minimum Eagle's medium with 5% fetal bovine serum and 2 mM glutamine. Cells were tested and found to be mycoplasma free.

Logarithmically growing cell populations in 100-mm plastic dishes (Becton Dickinson Labware, Franklin Lakes, NJ) were exposed to γ-rays at room temperature using a ^{137}Cs source at a rate of 2.6 Gy/min. Mock-treated control cells were subjected to the same movements both in and out of the incubators as treated cells, for both IR and *t*-butyl hydroperoxide treatments. When cells were treated with *t*-butyl hydroperoxide, the *t*-butyl hydroperoxide was added to cell cultures for 15 min. The cultures were then washed 2× with warm media, and the media were replaced. In experiments where some cell cultures were treated with *t*-butyl hydroperoxide, all plates within the same experiment were washed as described above. After treatment, the cells were incubated for the times indicated and harvested.

Cell Colony-forming Efficiency Assay—Logarithmically growing fibroblast populations were harvested by typsinization, counted in a cell counter (Coulter Counter ZM, Coulter Corp., Miami, Fl), and replated at a density of 10^3 fibroblasts/100-mm tissue culture dish. After allowing cells to adhere for 12 h, the fibroblasts were exposed for 15 min to various concentrations of *t*-butyl hydroperoxide, washed, and incubated for 8–12 days in appropriate media. For assays employing mannitol, fibroblasts were treated 1 h with 1 mM mannitol, followed by treatment with *t*-butyl hydroperoxide in the continued presence of 1 mM mannitol, washed, and incubated as described above. Media were removed and colonies fixed by the addition of water/methanol (1:1, v/v) containing crystal violet (1 g/liter) and counted using a dissecting microscope. For each fibroblast strain, a minimum of two colony-forming assay experiments was performed, with each data point done in triplicate.

Flow Cytometry for G_1 Checkpoint Function—G_1 checkpoint function was assayed by flow cytometry using a modification of the cell cycle analysis protocol in Kastan *et al*. (1) for simultaneous analysis of DNA synthesis and cell cycle. Logarithmically growing cells were either mock-treated, exposed to 3.0 Gy γ-IR, or exposed to various concentrations of *t*-butyl hydroperoxide as described above. 4 h following treatment, BrdUrd (Roche Molecular Biochemicals) was added to the media to a final concentration of 10 μM, and cells were incubated for an additional 2 h. Cells were harvested, fixed in phosphate-buffered saline (PBS)/methanol at a 1:2 (v/v) ratio, and stored at −20 °C. 5×10^5 cells from each sample were stained for BrdUrd incorporation in a solution of Tween 20/BSA plus anti-BrdUrd antibody (Becton Dickinson catalog number 347580) as recommended by the manufacturer. Fluorescein isothiocyanate-conjugated anti-mouse IgG antibody (Jackson ImmunoResearch Laboratories, West Grove, PA) was used as secondary antibody. Cells were stained with PBS containing 5 μg/ml propidium iodide (Roche Molecular Biochemicals) and analyzed using a Becton Dickinson FACSort. Twenty thousand cells were counted for each analysis. Flow cytometric experiments were done twice with each treatment point done in duplicate.

Protein Analysis and Histone H1 in Vitro Kinase Assays—After treatment, cells were harvested and solubilized on ice in kinase lysis buffer with inhibitors (10 mM sodium phosphate (pH 7.2), 150 mM NaCl, 1% Nonidet P-40, 1 mM EDTA, 5 mM EGTA, 5 mM β-glycerophosphate, 1 mM dithiothreitol, 120 kallikrein IU/ml aprotinin, and 10 μg/ml leupeptin). Protein concentration was determined using a detergent-compatible protein assay kit (Bio-Rad) with bovine serum albumin (BSA) as a standard. Although the amount of protein used in different kinase assay experiments varied, within each experiment the protein concentrations employed were the same for all samples. In $p34^{CDC2}$/cyclin B histone H1 *in vitro* kinase activity assays 50–100 μg of protein was used per kinase reaction, whereas 500–700 μg of protein was used per $p33^{CDK2}$/cyclin E histone H1 *in vitro* kinase assay. The desired amount of protein from solubilized extracts was aliquoted into 1.5-ml microcentrifuge tubes, and volumes were adjusted to 500 μl with kinase lysis buffer. The immunoprecipitations were done with either 0.5 μl of anti-human cyclin B Powerclonal antibody (catalog number 05-373, Upstate Biotechnology, Inc., Lake Placid, NY) or 2.0 μl of anti-human cyclin E Powerclonal antibody (catalog number 05-371, Upstate Biotechnology, Inc., Lake Placid, NY). Samples were precleared with protein G-agarose beads (Life Technologies, Inc.), then incubated with the primary antibody for 2 h, followed by the addition of protein G-agarose beads. Kinase reactions were carried out in histone H1 kinase buffer (20 mM HEPES (pH 7.3), 80 mM β-glycerophosphate, 20 mM EGTA, 50 mM $MgCl_2$, 5 mM $MnCl_2$, 1 mM dithiothreitol, 60 kallikrein IU/ml aprotinin, 10 μg/ml leupeptin, 10 μM cyclic AMP-dependent protein kinase-inhibitory peptide), with 8 μg of histone H1 and 10 μCi of [^{32}γ-P]ATP (3,000 Ci/mmol, Amersham Pharmacia Biotech) for 30 min at 37 °C. The kinase reactions were stopped by addition of 2× SDS sample buffer (4% SDS, 150 mM Tris (pH 6.8), 20% glycerol, 1 mM β-mercaptoethanol, 0.02% bromphenol blue), and proteins were resolved by 12% SDS-PAGE. Gels were stained with Coomassie Blue to verify equal histone protein loading, dried, and subjected to autoradiography with Hyperfilm MP (Amersham Pharmacia Biotech). The radiolabeled protein substrates in the dried gels were then quantified using a Molecular Dynamics PhosphorImager and ImageQuant software. All kinase assays were performed at least in triplicate.

Quantification of Mitotic Delay Induced by t-Butyl Hydroperoxide and IR—After appropriate treatment, fibroblasts were fixed on 100-mm dishes by the gentle addition of cold methanol. After 10 min the plates were air-dried and stored at 4 °C until staining with 0.2 μg/ml 4′,6-diamidino-2-phenylindole (DAPI). DAPI-stained cells then were examined by fluorescence microscopy. The percentage of mitotic cells (the mitotic index) was determined from counts of a minimum of 5,000 cells. All mitotic delay treatments were performed in duplicate, and all experiments were done in duplicate.

Protein Analyses—Immunoprecipitations of p53 were performed with whole cell extracts from five 100-mm tissue culture dishes (~800 μg protein/IP) as described above for protein kinase assays, using 2.5 μl of anti-p53 murine monoclonal antibody (catalog number OP03, Oncogene Research Products, Cambridge, MA) per sample. Eluted proteins were resolved by 12% SDS-PAGE and transferred to 0.2-μm nitrocellulose membranes. The blots were probed with anti-p53 antibody (a generous gift from Dr. B. Alex Merrick, NIEHS), which had been raised in rabbits against immunopurified human r-p53 expressed in a baculovirus expression system. By using anti-rabbit IgG peroxidase-conjugated goat antibody (Roche Molecular Biochemicals), p53 protein was visualized by chemiluminescence (Pierce) followed by exposure to Hyperfilm MP (Amersham Pharmacia Biotech). p53 immunoprecipitations and Western analysis were performed in triplicate.

To examine the effect of *t*-butyl hydroperoxide on HO-1 protein levels in normal and AT fibroblasts, we treated AT and NHF1 fibroblasts with 1–10 μM *t*-butyl hydroperoxide for 4 h. Cells were then harvested and lysed as described above; 100 μg of whole cell protein extract was loaded per lane; proteins were resolved by 12% SDS-PAGE and transferred to nitrocellulose membranes as described above. Nitrocellulose blots were probed with anti-HO-1 rabbit polyclonal antibody (catalog number PA3-019, Affinity Bioreagents, Golden, CO) and visualized using anti-rabbit IgG peroxidase-conjugated antibody (Roche Molecular Biochemicals) as described above. All HO-1 induction Western blots were done in triplicate.

Affinity Purification of pATM Antibody, αATM 7 a.p.—In order to isolate the highest affinity, highest specificity αATM 7 antibodies from the rabbit polyclonal antiserum, antibody was affinity-purified using the original peptide immunogen. Peptide corresponding to pATM residues 826–840 (ATM-N826 peptide) was immobilized to generate a peptide column in the following manner. Ten mg of ATM-N826 peptide were mixed with 1.0 ml of Affi-Gel 15 (Bio-Rad). The reaction mixture was mixed at room temperature for 2–3 h, and then the organic solvents were replaced with 10% ethanolamine in water for 1 h at room temperature to terminate the reaction and block any unreacted groups that remained. The derivatized Affi-Gel was poured into a column and cleaned by passing 4 M potassium thiocyanate through the packing. The column was washed with PBS and stored in PBS with 0.02% sodium azide at 4 °C.

To affinity-purify antipeptide antibody, IgG was isolated from the whole polyclonal rabbit serum using an Econo-Pac Protein A kit (Bio-Rad). Twenty five to 30 mg of the protein A-purified IgG was added to the Affi-Gel peptide column and tumbled overnight at 4 °C. The antibody-bound peptide beads were washed with 5 column volumes of 1 M potassium thiocyanate, and fractions were eluted with 4 M potassium thiocyanate. BSA (0.1%) was added to peak fractions prior to dialysis in

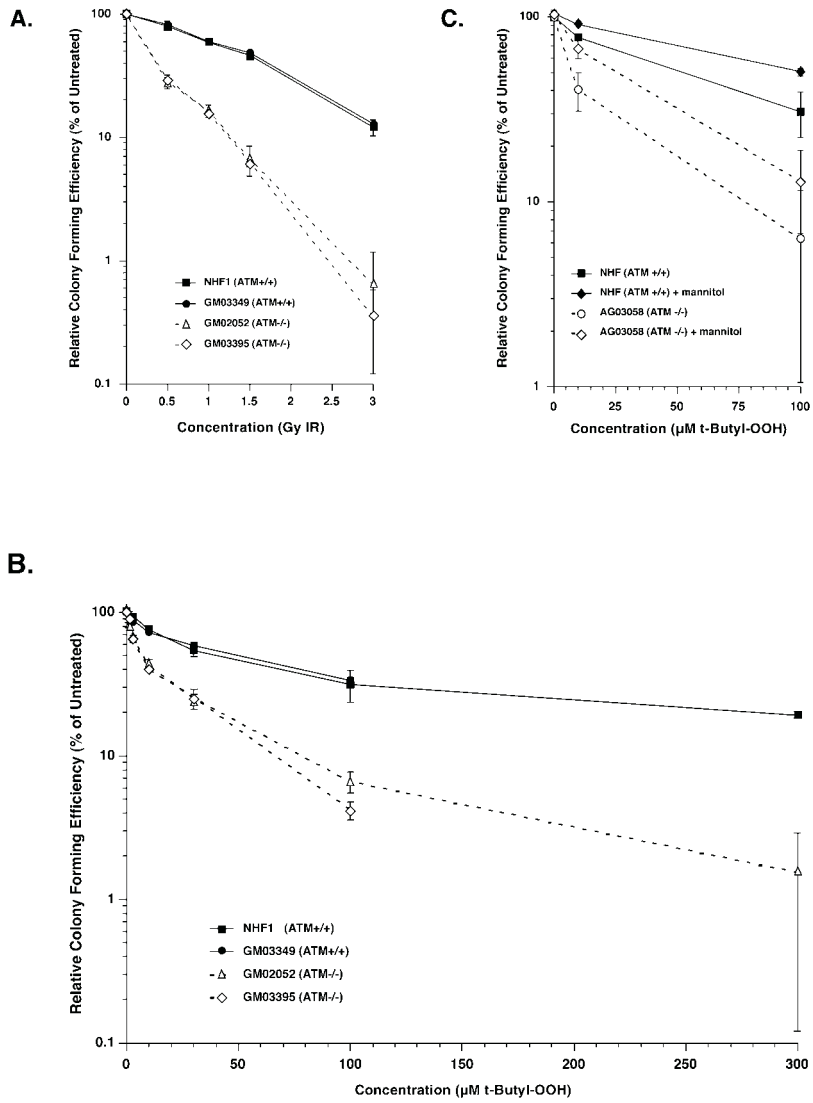

FIG. 1. **ATM-deficient cells are hypersensitive to killing following exposures to IR and *t*-butyl hydroperoxide.** *A,* the effect of increasing concentrations of IR on the colony-forming efficiency of two ATM-normal and two ATM-deficient fibroblasts. Exponentially growing fibroblasts were plated at a density of 10^3 cells/100-mm plate and allowed to adhere for 12 h. The cells were then treated with increasing concentrations of γ-IR and allowed to grow for 8–11 days. Cell colonies were then stained and counted. Data indicate survival as a percentage of untreated cells. *B,* the effect of increasing concentrations of *t*-butyl hydroperoxide on the colony-forming efficiency of two ATM-normal and two ATM-deficient fibroblast strains. Data indicate survival as a percentage of untreated cells. *C,* the effect of 1 mM mannitol on the colony-forming efficiency of the ATM-normal NHF1 and ATM-deficient AG03058 fibroblast stains after exposure to 10 and 100 μM *t*-butyl hydroperoxide. Data indicate survival as a percentage of untreated cells.

1× PBS overnight at 4 °C. The peak fractions were verified by Western blotting of total protein extracts from normal and *ATM*-deficient fibroblasts that had been resolved by 6% SDS-PAGE (acrylamide/bisacrylamide ratio of 100:1). Affinity-purified αATM 7 (αATM 7 a.p.) antibody was stored in 20% glycerol and 0.02% sodium azide at −20 °C.

pATM in Vitro PHAS-1 Kinase Assay—The pATM *in vitro* PHAS-1 kinase assays were done as described previously (16, 17). Cells were incubated for 90 min following exposure with 6.0 Gy γ-IR or a 15-min exposure to 300 μM *t*-butyl hydroperoxide and then lysed in kinase lysis buffer with 10 mM β-glycerophosphate and 1 mM $NaVO_3$ added. Cell lysates were clarified by centrifugation; the protein concentration was determined; the volume was adjusted to 0.9 ml with kinase lysis buffer plus inhibitors, and protein G-agarose beads were added to pre-clear the lysates as described above. After 30 min, the pre-cleared lysates were removed from the protein G-agarose beads and added to either 0.1 ml of kinase lysis buffer with inhibitors alone or containing αATM 7 a.p. antibody. In order to test antibody specificity, in some treatments the αATM 7 a.p. antibody was incubated for 30 min prior to its addition to the cell lysates with either 25 μg of the peptide that the antibody was raised against (ATM-N826) or with 25 μg of an irrelevant peptide sequence of the same length. All pATM kinase reactions were performed at least in triplicate using 1.5–3.0 mg protein lysate per immunoprecipitation.

Quantification of Thymine Glycol Formation in ATM-normal and ATM-deficient Fibroblasts after Treatment with t-Butyl Hydroperoxide and IR—To quantify the damage induced in NHFs and *ATM*-deficient fibroblasts by *t*-butyl hydroperoxide and IR, we measured thymine glycol formation in the DNA from *ATM*-normal NHF1 cells and *ATM*-deficient AG03058 fibroblasts following treatment by each agent. Six plates of logarithmically growing NHF1 or AG03058 fibroblasts, at ~70% confluence, were treated with 100 or 300 μM *t*-butyl hydroperoxide or 6 Gy γ-IR, as described above. Cells were harvested from each plate on ice with 5 ml of cold PBS as soon as possible following treatment. The cells were pelleted, washed 1 time in cold PBS, re-pelleted in 1.5-ml microcentrifuge tubes, and quick-frozen in dry ice/ethanol until assayed. Determination of thymine glycol formation was performed as described previously (29). Each experimental point was performed in triplicate.

RESULTS

AT Fibroblast Strains Are Hypersensitive to the Toxic Effects of t-Butyl Hydroperoxide—To examine the relative toxicity of reactive oxygen species exposure between normal and pATM-deficient fibroblasts, we treated different fibroblast strains with *t*-butyl hydroperoxide. We employed *t*-butyl hydroperoxide as a source of oxidative stress as it is poorly hydrolyzed by catalase (30). We reasoned that this is important since catalase activity has been reported to be low in *ATM*-deficient cells (31, 32) and thus, using a peroxide that can be hydrolyzed by catalase, would introduce experimental variation due to differences in cellular catalase activities.

To initiate these studies, two normal and two *ATM*-deficient fibroblast strains were treated with increasing levels of IR, and toxicity was assayed by colony-forming efficiency. As reported previously (7), exposure to increasing amounts of IR inhibited colony formation in *ATM*-deficient fibroblast strains more effectively than in NHFs (Fig. 1*A*). To compare the effects of *t*-butyl hydroperoxide on normal and *ATM*-deficient fibroblasts, normal NHF1 and GM03349 cells and *ATM*-deficient

TABLE I
Flow cytometric analysis of ATM-normal NHF1 and ATM-deficient AG03058 fibroblasts following treatment with increasing concentrations of t-butyl hydroperoxide (A) and 3.0 Gy IR (B)

Treatment/concentration	Relative percentage of cells in early S phase[a]	
	NHF1 (*ATM* +/+)	AG03058 (*ATM* −/−)
A. *t*-Butyl-OOH		
0 μM	100 (±8)[b]	100 (±8)
10 μM	100 (±7)	104 (±10)
30 μM	70 (±11)	117 (±4)
100 μM	54 (±5)	93 (±5)
B. γ-IR		
0 Gy	100 (±7)	100 (±7)
3.0 Gy	19 (±9)	96 (±6)

[a] Percentage of treated cells in early S phase relative to the percentage of mock-treated control cells in early S phase.
[b] ±, standard deviation.

GM02052 and GM03395 cells were treated with increasing concentrations of *t*-butyl hydroperoxide. As shown in Fig. 1*B*, the *ATM*-deficient fibroblasts were more sensitive to the colony-forming inhibiting effects of *t*-butyl hydroperoxide than the normal fibroblasts. LC_{50} (lethal concentration for 50% of population) for both normal fibroblast strains was in the 40–50 μM *t*-butyl hydroperoxide range, whereas the LC_{50} for the *ATM*-deficient dermal fibroblast strains was in the 6–8 μM range (Fig. 1*B*). The colony-inhibiting effect of *t*-butyl hydroperoxide in both normal and *ATM*-deficient fibroblast strains was biphasic, with an initial high sensitivity to low concentrations of *t*-butyl hydroperoxide (1–10 μM), followed by less sensitivity at higher concentrations (>10 μM). This apparent biphasic response is pATM-independent and suggests to us that higher concentrations of *t*-butyl hydroperoxide induce a pATM-independent resistance or adaptive response to the effects of *t*-butyl hydroperoxide in both cell types (Fig. 1*B*, compare 1–10 μM to 10–300 μM *t*-butyl hydroperoxide).

Peroxides are thought to exert some of their damaging effects through the production of reactive oxygen intermediates via events such as the Fenton reaction (for review see Ref. 33). We pretreated fibroblasts with mannitol for 1 h prior to *t*-butyl hydroperoxide treatment in order to ascertain if the colony-inhibiting effects of *t*-butyl hydroperoxide could be reduced by co-treatment with an antioxidant. Mannitol, which is effective at scavenging hydroxyl radicals (34), was used as an antioxidant. As shown in Fig. 1*C*, pretreatment with mannitol partially inhibited the killing effect of *t*-butyl hydroperoxide on both normal and *ATM*-deficient fibroblast strains. For most concentrations examined, the differences between treatment with and without mannitol are significant. However, pretreatment with mannitol of the *ATM*-deficient cells showed less reduction of killing following treatment with the highest concentration of *t*-butyl hydroperoxide (100 μM) (Fig. 1*C*). This is likely to be due to the very low number of *ATM*-deficient cells that can still form colonies at this concentration of *t*-butyl hydroperoxide. Nevertheless, these data show that the toxic effect of *t*-butyl hydroperoxide can be partially reversed by pretreatment with an antioxidant.

Fibroblasts Lacking pATM Function Fail to Exhibit G_1 Checkpoint Delay in Response to t-Butyl Hydroperoxide Exposure—G_1 checkpoint function, as reflected by delay of entry into S phase, was assayed following exposure to oxidative stress. Exposure of NHF1 fibroblasts in logarithmic growth phase to *t*-butyl hydroperoxide over a 10–100 μM range resulted in a concentration-dependent suppression of S phase entry, as measured by flow cytometry (Table I and Fig. 2). When the *ATM*-deficient fibroblast strain AG03058 was subjected to the same treatment, comparatively little inhibition of S phase entry was observed over the same concentrations of *t*-butyl hydroperoxide (Table I and Fig. 2). As demonstrated previously (11, 35), normal fibroblasts exhibit G_1 checkpoint arrest in response to IR, whereas *ATM*-deficient fibroblasts did not (Table I and Fig. 2).

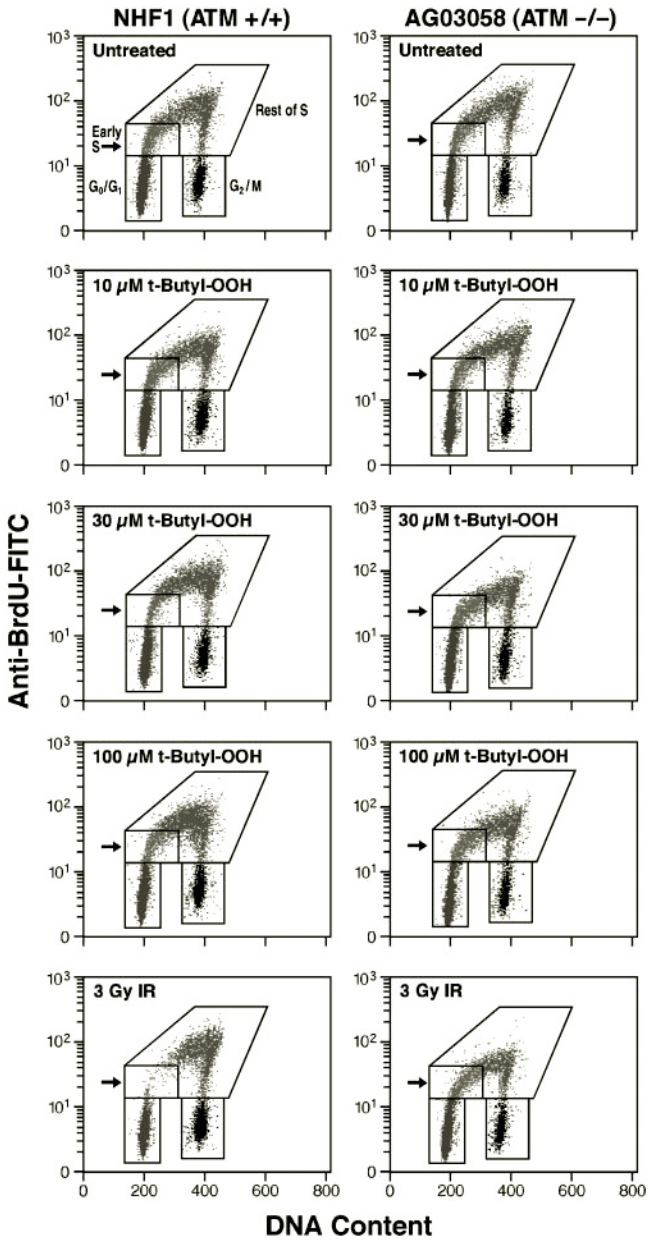

FIG. 2. **Flow cytometric analysis of G_1 checkpoint delay in response to *t*-butyl hydroperoxide exposure and IR treatment in *ATM*-normal NHF1 and *ATM*-deficient AG03058 fibroblasts.** Exponentially growing cells were treated as indicated. Four hours after treatment, BrdUrd (*BrdU*) was added for the last 2 h of incubation. Cells were fixed and stained with α-BrdUrd-fluorescein isothiocyanate and propidium iodide. *Dot plots* show incorporation of BrdUrd into DNA as an indication of DNA synthesis and propidium iodide fluorescence as an indication of DNA content. The regions drawn represent areas from which data were taken for analysis.

p53 protein stabilization and activation, which is necessary for the elicitation of a full G_1 checkpoint response to cellular damage from IR exposure for more than a transient period (36–38), is severely attenuated in *ATM*-deficient cells (35–37). Since *ATM*-deficient cells exhibit poor p53 induction in response to IR and fail to show a G_1 checkpoint function in response to both IR and *t*-butyl hydroperoxide treatment, we hypothesized that p53 induction in response to *t*-butyl hydroperoxide treatment would similarly be poor in AT fibro-

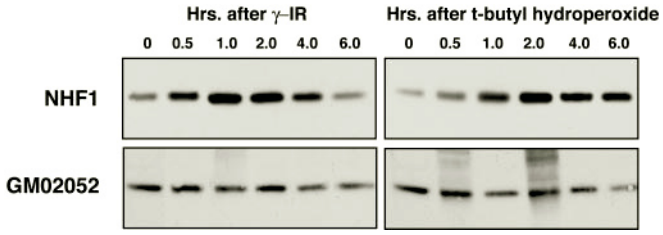

FIG. 3. **Western blot of p53 shows induction in response to *t*-butyl hydroperoxide or γ-IR treatment in normal and *ATM*-deficient fibroblasts.** Cells were treated as indicated. p53 was immunoprecipitated with an anti-p53 antibody, and SDS-PAGE was performed. The resolved proteins were transferred to nitrocellulose paper and probed with a second anti-p53 antibody.

blasts compared with NHFs. When p53 immunoprecipitations were performed, followed by Western blotting with a second anti-p53 antibody, we found that p53 was induced in NHF1 cells in response to both *t*-butyl hydroperoxide and IR (Fig. 3). p53 induction in response to *t*-butyl hydroperoxide was slower than induction in response to IR, with significant induction following IR exposure by 1 h and induction by *t*-butyl hydroperoxide peaking later, ~1–2 h (Fig. 3). At the time points examined here, neither IR nor *t*-butyl hydroperoxide treatment significantly induced p53 protein levels in the *ATM*-deficient fibroblast strain GM02052 (Fig. 3).

$p33^{CDK2}$/cyclin E-associated kinase activity has been shown to be required for progression through late G_1 and into S phase (39). To test the effect of *t*-butyl hydroperoxide on $p33^{CDK2}$/cyclin E-associated kinase activity, we treated the NHF1 fibroblast strain with either 300 μM *t*-butyl hydroperoxide or 3.0 Gy IR, followed by incubation for 1–10 h, and we measured $p33^{CDK2}$/cyclin E histone H1 *in vitro* kinase activity. As shown in Fig. 4, both treatments resulted in $p33^{CDK2}$/cyclin E histone H1 *in vitro* kinase activity suppression. Maximal inhibition occurred at 6 h, followed by partial recovery at 10 h. The inhibition observed following treatment of NHF1 cells with 300 μM *t*-butyl hydroperoxide was less than that with exposure to 3.0 Gy IR and occurred with delayed kinetics compared with IR treatment (compare Fig. 4, *A* and *B*). When NHF1 cells were treated with *t*-butyl hydroperoxide over a 10 μM to 1 mM range and incubated for 6 h, $p33^{CDK2}$/cyclin E histone H1 *in vitro* kinase activity was found to fall in a concentration-dependent manner, with kinase activity reduced ~70% at concentrations of 100 μM *t*-butyl hydroperoxide and above (data not shown). When the *ATM*-deficient dermal fibroblast strain GM02052 was treated with 300 μM *t*-butyl hydroperoxide or 3.0 Gy, followed by incubation for 1–10 h, the *ATM*-deficient fibroblasts failed to exhibit significant inhibition of kinase activity by either agent (Fig. 4, *A* and *B*).

t-Butyl Hydroperoxide Exposure Induces a G_2 Checkpoint Response in Normal Fibroblasts That Is Defective in Fibroblasts Lacking pATM Function—Exposure of logarithmically growing cells from the normal fibroblast strain NHF1 to 1.5 Gy IR resulted in a rapid delay of entry into mitosis 2 h post-treatment, with a reduction in the mitotic index to only 3% (±10%) that of the mock-treated cells. *ATM*-deficient fibroblast cells (GM02052) showed no significant reduction in the mitotic index relative to mock-treated controls (94 ± 2%), in agreement with previous findings (40). Similarly, exposure of NHF1 cells to 10–300 μM *t*-butyl hydroperoxide generated a strong G_2 checkpoint response (Fig. 5). Under the same conditions over the same concentration range of *t*-butyl hydroperoxide treatment, no significant inhibition of entry into mitosis was observed with the *ATM*-deficient fibroblast strain cells (GM02052) 2 h post-treatment (Fig. 5).

To explore further the G_2 checkpoint response to *t*-butyl

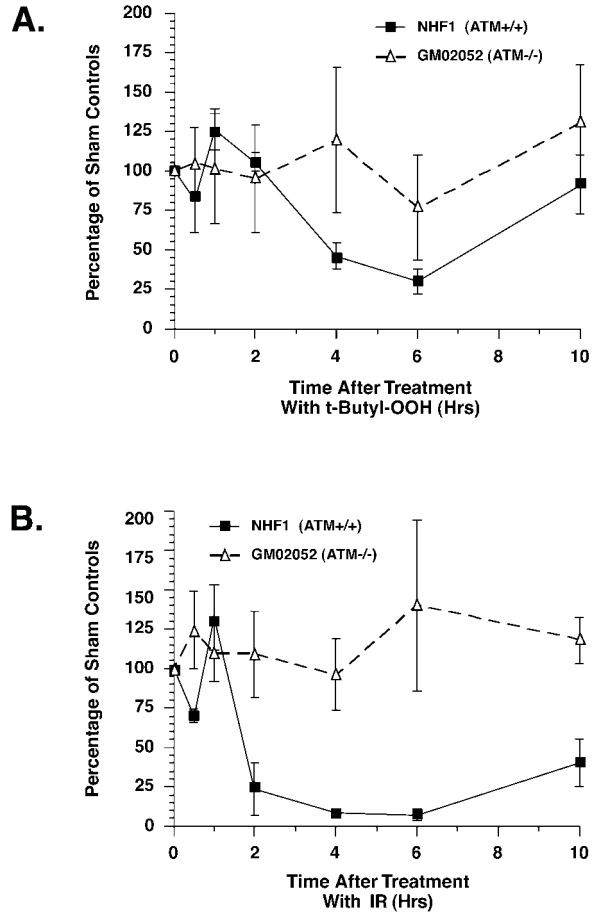

FIG. 4. **Time course showing the effect of *t*-butyl hydroperoxide and IR treatment on $p33^{CDK2}$/cyclin E kinase activity in a normal and *ATM*-deficient fibroblast strain.** Cells in log phase were exposed for 15 min to 300 μM *t*-butyl hydroperoxide (*A*) or exposed to 3.0 Gy γ-IR (*B*). The cells were then cultured for the indicated times, lysed, and immunoprecipitated with anti-cyclin E antibody to obtain $p33^{CDK2}$/cyclin E protein complexes following the addition of protein G-agarose beads. $p33^{CDK2}$/cyclin E kinase activity was measured by *in vitro* kinase assay using exogenous histone H1 protein as the substrate in the presence of [γ-^{32}P]ATP. SDS-PAGE was performed to resolve proteins; the gel was dried, and kinase activity was quantified by phosphorimaging.

hydroperoxide treatment, we performed $p34^{CDC2}$/cyclin B histone H1 *in vitro* kinase activity assays on protein extracts from two normal and two *ATM*-deficient fibroblast strains. As shown in Fig. 6*A*, $p34^{CDC2}$/cyclin B histone H1 *in vitro* kinase activity was suppressed in a concentration-dependent manner 2 h post-treatment with 1–300 μM *t*-butyl hydroperoxide in both normal human fibroblast strains, NHF1 and GM03349. Similarly, exposure to 1.5 Gy IR inhibited $p34^{CDC2}$/cyclin B histone H1 *in vitro* kinase activity from normal human fibroblasts, as we have previously reported (40, 41) (Fig. 6*B*). Neither treatment with *t*-butyl hydroperoxide at any concentration nor exposure to 1.5 Gy IR caused the two *ATM*-deficient fibroblast strains, GM02052 and GM03395, to display a significant suppression of $p34^{CDC2}$/cyclin B histone H1 *in vitro* kinase activity (Fig. 6, *A* and *B*). A representative $p34^{CDC2}$/cyclin B histone H1 *in vitro* kinase assay for NHF1 and GM02052 fibroblasts is shown in Fig. 6*C*.

To investigate the possibility that the *ATM*-deficient fibroblast strains were capable of exhibiting a G_2 checkpoint function but with delayed kinetics in response to exposures of *t*-butyl hydroperoxide, a time course analysis of $p34^{CDC2}$/cyclin B histone H1 *in vitro* kinase activity following treatment was performed. The results indicate that treatment with 300 μM

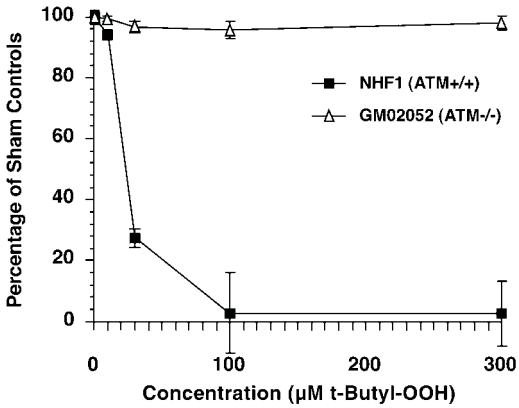

FIG. 5. **Analysis of the delay of mitotic entry following exposure to different concentrations of *t*-butyl hydroperoxide in the *ATM*-normal NHF1 and *ATM*-deficient GM02052 fibroblasts.** Cells were treated as indicated, fixed by the addition of cold methanol, and stained with DAPI. The percentage of mitotic cells was counted by fluorescence microscopy. The results are expressed as the relative mitotic index, which is the mitotic index of the treated population expressed as a percentage of the mitotic index of the mock-treated population.

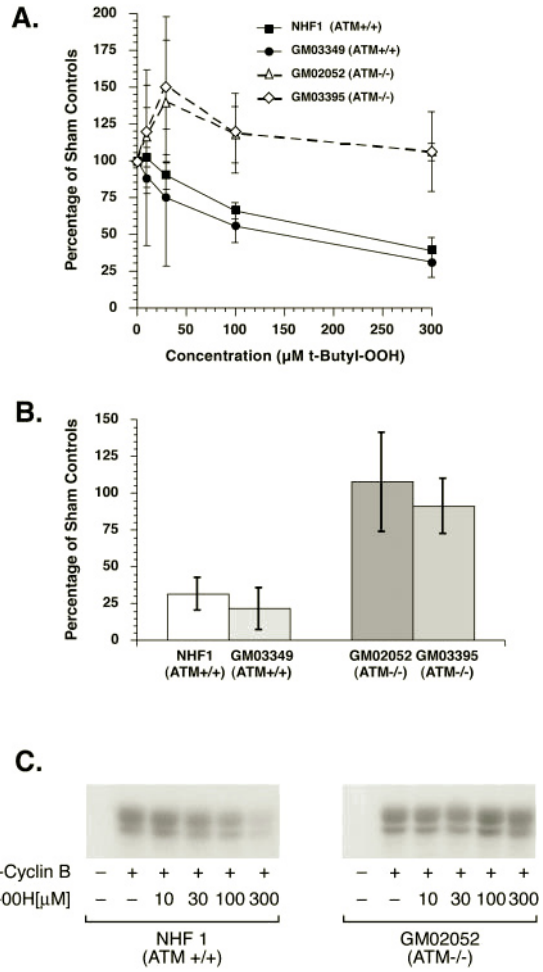

FIG. 6. **Concentration-response curve showing the effect of *t*-butyl hydroperoxide and γ-IR treatment on p34^{CDC2}/cyclin B1 kinase activity in two *ATM*-normal and two *ATM*-deficient fibroblast strains.** Cells were harvested for analysis 2 h following treatment with either increasing concentrations of *t*-butyl hydroperoxide (*A*) or 1.5 Gy γ-radiation (*B*). Cyclin B1-associated kinase activity was analyzed by immunoprecipitation of protein with anti-cyclin B1 antibody, followed by *in vitro* kinase analysis using histone H1 as an exogenous substrate. *C* shows a representative p34^{CDC2}/cyclin B1 kinase assay with pATM-normal NHFs and pATM-deficient GM02052 fibroblasts. Proteins were resolved by SDS-PAGE, and incorporation of γ-^{32}P into histone H1 protein was quantified by PhosphorImager analysis.

t-butyl hydroperoxide and exposure to 1.5 Gy IR were both effective at suppressing p34^{CDC2}/cyclin B histone H1 kinase activity in NHF1 cells at 1 h post-treatment, with maximal suppression of kinase activity occurring at 2 h. Activity recovered to roughly untreated levels by 6 h (Figs. 7, *A* and *B*). These kinetics closely resemble those reported previously for the suppression of mitotic entry by 1.5 Gy IR (40). Neither *ATM*-deficient fibroblast strain (GM02052 and GM03395) showed significant suppression of p34^{CDC2}/cyclin B histone H1 *in vitro* kinase activity in response to either treatment with 300 μM *t*-butyl hydroperoxide or exposure to 1.5 Gy IR at any time points examined (Fig. 7, *A* and *B*). Mannitol pretreatment reduced the p34^{CDC2}/cyclin B histone H1 *in vitro* kinase activity inhibition initiated by 100 μM *t*-butyl hydroperoxide treatment (data not shown). Thus an antioxidant may partially reverse the suppressive effects of *t*-butyl hydroperoxide on the G_2 checkpoint function as indicated by the inhibition of p34^{CDC2}/cyclin B kinase activity.

t-Butyl Hydroperoxide Treatment Activates pATM-associated Kinase Activity—IR treatment of melanoma and lymphoblast cell lines was found to increase pATM-associated kinase activity toward the PHAS-1 and p53 proteins in *in vitro* kinase activity assays (16, 17). IR-inducible kinase activity was found in pATM normal cell lines but not in cells lines derived from AT patients. In these studies, pATM kinase activity was reported to be induced by roughly 2-fold following treatment with IR (16, 17). Based on the data above, we hypothesized that oxidative damage generated by treatment with *t*-butyl hydroperoxide should induce pATM-associated kinase activity.

A rabbit polyclonal antiserum to a peptide corresponding to pATM residues 826–840 was raised and affinity-purified to the cognate peptide. Based on Western blot analysis of whole cell and/or nuclear protein extracts from NHF1 and HeLa cells, it was determined that the anti-ATM 7 affinity-purified antibody (αATM 7 a.p.) recognizes a protein of ~350 kDa, the predicted size of pATM. This band was not detected in dermal fibroblasts derived from individuals with AT (Fig. 8).

NHF1 cells and the *ATM*-deficient dermal fibroblast strain AG03058 treated with either 6.0 Gy IR or 15 min with 300 μM *t*-butyl hydroperoxide were examined for pATM kinase activity 90 min following treatment. As shown in Fig. 9*A*, low levels of pATM-associated *in vitro* kinase activity were found to be associated with immunoprecipitated protein complexes from extracts from untreated NHFs using the αATM 7 a.p. antibody. This activity was roughly 50% higher than the background level of kinase activity associated with protein G-agarose bead mock immunoprecipitations (using no antibody) with extracts from IR-treated NHFs. When protein extracts from NHF1 cells treated with either IR or *t*-butyl hydroperoxide were assayed for pATM-associated *in vitro* kinase activity toward PHAS-1 protein, the level of activity in the immunocomplexes was significantly increased. *t*-Butyl hydroperoxide treatment induced pATM-associated kinase activity an average of 2.2-fold over the level found associated with pATM immunocomplexes from untreated NHF1 cells in 3 independent experiments. IR treatment increased pATM-associated kinase activity an average of 2.1-fold (average of 6 independent experiments) (Fig. 9*A*). A representative pATM kinase assay is shown in Fig. 9*B*. To examine the pATM-dependent specificity of these *in vitro* kinase assays, αATM 7 a.p. antibody was preincubated with either the peptide that it was raised against (ATM-N826) or an irrelevant peptide of the same length (data not shown). As shown in Fig. 9*A*, the ATM-N826 peptide largely blocked IR-

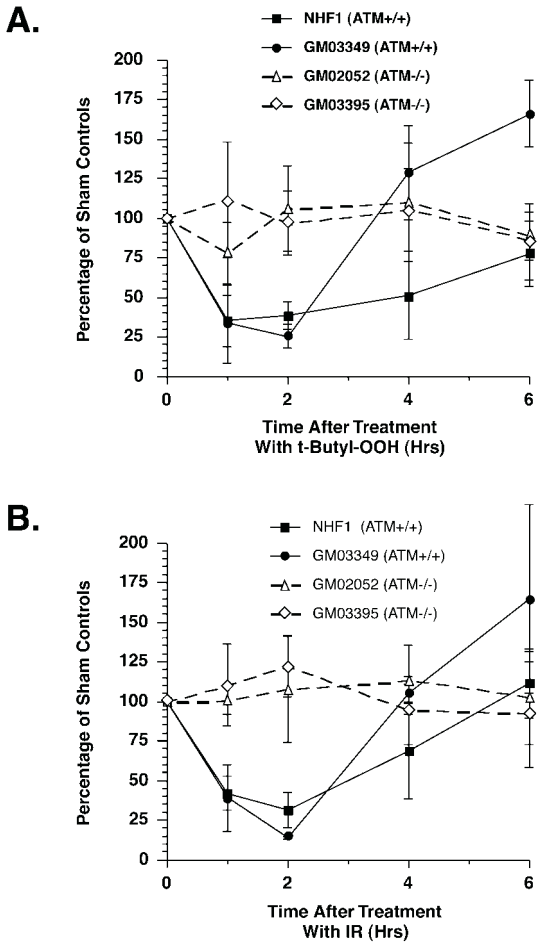

FIG. 7. **Time course showing the effect of *t*-butyl hydroperoxide and γ-IR treatment on p34^{CDC2}/cyclin B1 kinase activity in two *ATM*-normal and two *ATM*-deficient fibroblast strains.** Cells were exposed to either 300 μM *t*-butyl hydroperoxide (*A*) or 1.5 Gy γ-radiation (*B*) and harvested at the indicated times. Cyclin B1-associated kinase activity was analyzed using histone H1 as an exogenous substrate.

FIG. 8. **pATM Western analysis.** HeLa cells, NHF1 cells, and two dermal fibroblast strains from individuals with AT were analyzed by immunoblot analysis for pATM. Whole cell extracts were prepared and subjected to SDS-PAGE followed by transblotting onto nitrocellulose. The blots were then probed for pATM using αATM 7 a.p., a rabbit polyclonal antibody that was peptide affinity-purified.

induced pATM-associated *in vitro* kinase activity to PHAS-1. Finally, pretreatment with 1 mM mannitol significantly lowered *t*-butyl hydroperoxide-induced pATM-associated kinase activity toward the PHAS-1 protein (data not shown), indicating that an antioxidant could reverse the pATM-activating effects of *t*-butyl hydroperoxide in this assay.

Further confirmation that the *in vitro* kinase activity toward PHAS-1 was associated with pATM was found in that *in vitro* kinase activity assayed from protein extracts from fibroblasts lacking pATM showed no significant difference whether anti-pATM antibody was present in the assays or not. Furthermore, with extracts from IR- or *t*-butyl hydroperoxide-treated *ATM*-deficient fibroblasts, the addition of ATM-N826 peptide to the assay did not suppress the background level of *in vitro* kinase activity (Fig. 9*B*).

Heme Oxygenase-1 Induction Is Normal in AT Fibroblasts—Heme oxygenase-1 (HO-1) is induced in human skin fibroblasts by peroxides (42). To determine whether AT fibroblasts were deficient in this response to oxidative stress, we treated four fibroblast strains (1 normal and 3 from individuals with AT) with 0, 1, 3, 10, 30, and 100 μM *t*-butyl hydroperoxide for 4 h and performed Western blot analysis for HO-1 protein. As shown in Fig. 10, *t*-butyl hydroperoxide treatment resulted in an induction of HO-1 protein at 10 μM concentrations and above in all four fibroblast strains. There was no significant difference in the response of any of the fibroblasts to HO-1 induction. Western blot analyses demonstrated that *t*-butyl hydroperoxide maximally induced HO-1 protein at 4–5 h in each cell type (data not shown). Pretreatment of NHF1 fibroblasts with mannitol for 1 h followed by treatment with 10 μM *t*-butyl hydroperoxide for 4 h in the continued presence of mannitol resulted in a significant inhibition of HO-1 protein induction, demonstrating that an antioxidant could partially reverse the effects of *t*-butyl hydroperoxide (data not shown).

Thymine Glycol Formation Induced by t-Butyl Hydroperoxide Treatment Is the Same in pATM-normal and pATM-deficient Fibroblasts—NHF1 cells and *ATM*-deficient fibroblasts (AG03058) were treated with *t*-butyl hydroperoxide or IR and examined for thymine glycol formation. As shown in Table II, treatment of either fibroblast type with 100 or 300 μM *t*-butyl hydroperoxide (A) or 6.0 Gy γ-IR (B) resulted in essentially equal thymine glycol formation between the fibroblast types. Thus, the initial damage produced by *t*-butyl hydroperoxide and IR treatment in pATM normal and deficient fibroblasts is not significantly different, as measured by thymine glycol formation.

DISCUSSION

We have examined the role of pATM in cellular responses to oxidative damage generated by *t*-butyl hydroperoxide treatment of normal human fibroblasts and *ATM*-deficient dermal fibroblasts. We undertook this study for several reasons as follows. 1) *ATM*-deficient cells have been reported to be unusually sensitive to oxidants such as nitric oxide, superoxide, and hydrogen peroxide in colony-forming efficiency assays compared with normal cells (21, 23–25). 2) *ATM*-deficient cells re-synthesize glutathione unusually slowly after depletion with diethyl maleate (22). 3) Cellular damage by IR exposure has been suggested to involve damage due to reactive oxygen species (43). 4) The *RAD9* gene product, which has similar functions to pATM, has been found to be necessary for checkpoint arrest in response to peroxide exposure (44). 5) BRCA1, which has been demonstrated to play a role in protecting cells from damage by hydrogen peroxide (45), has recently been found to

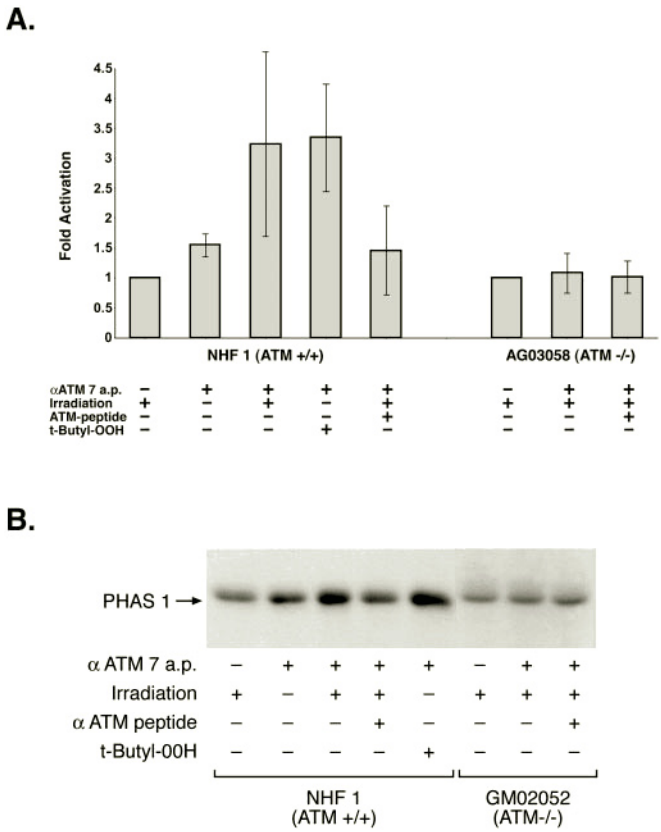

FIG. 9. **pATM *in vitro* kinase assay.** *A,* NHFs (*ATM*-normal) and the *ATM*-deficient dermal fibroblasts AG03058 were treated with either 300 μM *t*-butyl hydroperoxide or 6.0 Gy γ-IR, as indicated, incubated for 90 min, then harvested, and lysed, and protein extracts were subjected to immunoprecipitation with αATM 7 a.p. antibody. An *in vitro* kinase analysis was performed using PHAS-1 protein as an exogenous substrate in the presence of [γ-^{32}P]ATP. *Error bars* in this figure represent standard deviation in three successive pATM *in vitro* kinase assays. The incorporation of γ-^{32}P into PHAS-1 protein was quantified by SDS-PAGE followed by PhosphorImager analysis. *B,* a representative pATM *in vitro* kinase assay used to generate figure *A*. The relative values of each data point are as follows: *1st lane,* 1.00 ± 0; *2nd lane*, 1.55 ± 0.19; *3rd lane*, 3.24 ± 1.54; *4th lane*, 3.35 ± 0.90; *5th lane*, 1.46 ± 0.75; *6th lane*, 1.00 ± 0; *7th lane*, 1.08 ± 0.33; and *8th lane*, 1.02 ± 0.27, where assays with extracts from γ-irradiated cells plus protein G-agarose beads without any antibody were set at 1.00 in each experiment.

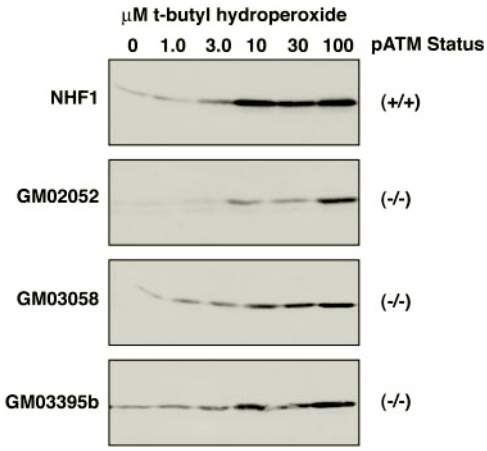

FIG. 10. **Western blot analysis of heme oxygenase induction in response to *t*-butyl hydroperoxide treatment.** One normal and three *ATM*-deficient fibroblast strains were treated as indicated; whole cell lysates were prepared, and protein extracts were subjected to SDS-PAGE. The resolved proteins were then transblotted onto nitrocellulose and probed using an anti-heme oxygenase antibody.

TABLE II
Thymine glycol formation in ATM-normal NHF1 and ATM-deficient AG03058 fibroblasts following treatment with 100 and 300 μM t-butyl hydroperoxide and 6.0 Gy γ-IR

Treatment/concentration	Thymine glycol/10^7 bases[a]	
	NHF1 (*ATM* +/+)	AG03058 (*ATM* −/−)
A. t-Butyl-OOH		
0 μM	ND[b]	ND
100 μM	19 (±3)[c]	20 (±2)
300 μM	60 (±4)	58 (±4)
B. γ-IR		
6.0 Gy	5.5 (±0.3)	5.5 (±0.2)

[a] Cells were harvested immediately after treatment and quick-frozen until analysis. Thymine glycol quantification was performed as reported previously (29).
[b] ND, not detectable.
[c] ±, standard deviation.

be phosphorylated by activated pATM (46). 6) *ATM*-deficient mice have been found to have elevated markers of oxidative damage, such as nitrotyrosine and hemeoxygenase activity, in organs known to be affected by the AT phenotype. Interestingly, cerebellar HO levels were found to be 600% greater in *ATM*-deficient mice than in *ATM*-normal mice (26). This last observation is particularly interesting as cerebellar pathologies are a hallmark of AT (47–49). Finally, pATM has been suggested to function, in part, as a sensor of oxidative stress (20).

We report that compared with pATM normal fibroblasts, *ATM*-deficient fibroblasts exhibit the following characteristics after oxidative damage: 1) greater sensitivity to the toxic effects of *t*-butyl hydroperoxide treatment in colony-forming efficiency assays; 2) failure to delay late G_1 phase progression, as measured by flow cytometry; 3) failure to exhibit G_1 checkpoint function, as measured by inhibition of $p33^{CDK2}$/cyclin E-associated *in vitro* kinase activity; 4) failure to induce p53; 5) failure to exhibit inhibition of $p34^{CDC2}$/cyclin B histone H1 *in vitro* kinase activity; and 6) failure to delay entry into mitosis. Also *t*-butyl hydroperoxide stimulates pATM-associated kinase activity. Thus, in response to oxidative damage, *ATM*-deficient cells appear to lack many critical cell cycle checkpoint responses, in a similar manner to that observed with IR-induced damage (for review see Ref. 33).

In contrast to these findings, HO-1 protein induction in response to *t*-butyl hydroperoxide appeared normal in *ATM*-deficient fibroblasts, indicating that some cellular responses to oxidative damage are regulated normally in *ATM*-deficient cells. Similarly, both *ATM*-deficient and -normal cells exhibited a biphasic response in colony-forming efficiency assays, with an initial sensitivity to low concentrations of *t*-butyl hydroperoxide (1–10 μM), followed by lesser sensitivity at higher concentrations (>10 μM). Whereas *ATM*-deficient fibroblasts were clearly more sensitive to the colony-forming inhibitory effects of *t*-butyl hydroperoxide, the appearance of the biphasic response in both normal and AT cells suggests that higher concentrations of *t*-butyl hydroperoxide (>10 μM) induce a resistance to the effects of *t*-butyl hydroperoxide that is both pATM-independent and similar to that seen in normal cells. The biphasic colony-inhibitory response we found here is similar to one reported with mouse embryonic stem cells exposed to hydrogen peroxide (45), suggesting that this biphasic response may be a common adaptive event following peroxide exposure.

One possible interpretation of our findings could be that *ATM*-deficient cells may respond normally to oxidative damage generated by *t*-butyl hydroperoxide treatment but not exhibit normal checkpoint responses or p53 induction due to their receiving less damage than normal fibroblasts after exposure to the same concentration of *t*-butyl hydroperoxide. To address

this issue we quantified DNA damage induced by IR and *t*-butyl hydroperoxide exposure by quantifying thymine glycol formation in normal and *ATM*-deficient fibroblasts. We found that thymine glycol formation was not significantly different between the fibroblast types directly following exposure to either agent. Based on these data, we conclude that the initial damage received by normal and *ATM*-deficient fibroblasts following IR and *t*-butyl hydroperoxide exposure is approximately the same and that, in fact, it is the absence of pATM function that accounts for the differences seen between the cells types.

A major hallmark of cells from individuals with AT is the ablation of the G_1, S, and G_2 checkpoint functions in response to IR, as well as other IR response-related events, such as p53 and p21 induction (11, 12, 36, 37, 50). Here we have shown that after exposure to *t*-butyl hydroperoxide, *ATM*-deficient fibroblasts lack G_1 and G_2 checkpoint responses, lack p53 induction, and show enhanced toxicity, reminiscent of the cellular responses seen with *ATM*-deficient fibroblasts exposed to IR. Thus our data support the hypothesis that pATM plays a role in resistance to oxidative stress (20).

Cell cycle checkpoints are thought to function, in part, to allow cells time to repair damage, particularly damage to DNA, before re-entering the cell cycle and completing subsequent cellular events such as DNA replication or mitosis. Ablation of cellular checkpoint functions, such as occurs in *ATM*-deficient cells or in cells treated with methylxanthines, can result in greater lethality following exposure to toxic agents (for review see Ref. 33). One question we have not addressed is whether or not pATM responds to oxidative damage to DNA or responds directly to a change in intracellular redox state independent of DNA damage. Although our data do not address this question specifically, we do demonstrate that *ATM*-deficient fibroblasts fail to exhibit normal G_1 and G_2 checkpoint responses following exposure to oxidative stress. Thus the inability of *ATM*-deficient cells to exhibit G_1 and G_2 checkpoint responses following oxidative damage is likely to be one mechanism that predisposes these cells to enhanced toxicity in response to exposure to oxidative stress. Our results suggest that there is an inability to respond to oxidative stress in cells from individuals with AT, a consequence of which may be relevant to the mechanisms of Purkinje cell death and other pathological changes observed in AT patients.

Acknowledgments—We thank B. Alex Merrick for the generous provision of p53 antibody, and Bradley Sturgeon, Chia Chiao, and Cynthia Afshari for their many helpful discussions and suggestions.

REFERENCES

1. Kastan, M. B., Onyekere, O., Sidransky, D., Volgelstein, B., and Craig, R. W. (1991) *Cancer Res.* **51,** 6304–6311
2. Broeks, A., Urbanus, J. H., Floore, A. N., Dahler, E. C., Klijn, J. G., Rutgers, E. J., Devilee, P., Russell, N. S., van Leeuwen, F. E., and van't Veer, L. J. (2000) *Am. J. Hum. Genet.* **66,** 494–500
3. Swift, M., Morrell, D., Massey, R. B., and Chase, C. L. (1991) *N. Engl. J. Med.* **325,** 1831–1836
4. Meyn, M. S. (1993) *Science* **260,** 1327–1330
5. Easton, D. F. (1994) *Int. J. Radiat. Biol.* **66,** 177–182
6. Painter, R. B., and Young, B. R. (1976) *Biochim. Biophys. Acta* **418,** 146–153
7. Shiloh, Y., Tabor, E., and Becker, Y. (1982) *Exp. Cell Res.* **140,** 191–199
8. Scott, D., Spreadborough, A. R., and Roberts, S. A. (1994) *Int. J. Radiat. Biol.* **66,** 157–163
9. Gatti, R. A., Berkel, I., Boder, E., Braedt, G., Charmley, P., Concannon, P., Ersoy, F., Foroud, T., Jaspers, N. G., Lange, K., Lathrop, G. M., Leppert, M., Nakamura, Y., O'Connell, P., Paterson, M., Salser, W., Sanal, O., Silver, J., Sparkes, R. S., Susi, E., Weeks, D. E., Wei, S., White, R., and Yoder, F. (1988) Nature **336,** 577–580
10. McKinnon, P. J. (1987) *Hum. Genet.* **75,** 197–208
11. Painter, R. B., and Young, B. R. (1980) *Proc. Natl. Acad. Sci. U. S. A.* **77,** 7315–7317
12. Zampetti-Bosseler, F., and Scott, D. (1981) *Int. J. Radiat. Biol.* **39,** 547–558
13. Beamish, H., and Lavin, M. F. (1994) *Int. J. Radiat. Biol.* **65,** 175–184
14. Paules, R. S., Levedakou, E. N., Wilson, S. J., Innes, C. L., Rhodes, N., Tlsty, T. D., Galloway, D. A., Donehower, L. A., Tainsky, M. A., and Kaufmann, W. K. (1995) *Cancer Res.* **55,** 1763–1773
15. Savitsky, K., Barshira, A., Gilad, S., Rotman, G., Ziv, Y., Vanagaite, L., Tagle, D. A., Smith, S., Uziel, T., Sfez, S., Ashkenazi, M., Pecker, I., Frydman, M., Harnik, R., Patanjali, S. R., Simmons, A., Clines, G. A., Sartiel, A., Gatti, R. A., Chessa, L., Sanal, O., Lavin, M. F., Jaspers, N. G. J., Malcolm, A., Taylor, R., Arlett, C. F., Miki, T., Weissman, S. M., Lovett, M., Collins, F. S., and Shiloh, Y. (1995) *Science* **268,** 1749–1753
16. Banin, S., Moyal, L., Shieh, S. Y., Taya, Y., Anderson, C. W., Chessa, L., Smorodinsky, N. I., Prives, C., Reiss, Y., Shiloh, Y., and Ziv, Y. (1998) *Science* **281,** 1674–1677
17. Canman, C. E., Lim, D. S., Cimprich, K. A., Taya, Y., Tamai, K., Sakaguchi, K., Appella, E., Kastan, M. B., and Siliciano, J. D. (1998) *Science* **281,** 1677–1679
18. Keith, C. T., and Schreiber, S. L. (1995) *Science* **270,** 50–51
19. Savitsky, K., Sfez, S., Tagle, D. A., Ziv, Y., Sartiel, A., Collins, F. S., Shiloh, Y., and Rotman, G. (1995) *Hum. Mol. Genet.* **4,** 2025–2032
20. Rotman, G., and Shiloh, Y. (1997) *BioEssays* **19,** 911–917
21. Vuillaume, M. (1987) *Mutat. Res.* **186,** 43–72
22. Meredith, M. J., and Dodson, M. L. (1987) *Cancer Res.* **47,** 4576–4581
23. Vuillaume, M., Best-Belpomme, M., Lafont, R., Hubert, M., Decroix, Y., and Sarasin, A. (1989) *Carcinogenesis* **10,** 1375–1381
24. Ward, A. J., Olive, P. L., Burr, A. H., and Rosin, M. P. (1994) *Environ. Mol. Mutagen.* **24,** 103–111
25. Green, M. H. L., Marcovitch, A. J., Harcourt, S. A., Lowe, J. E., Green, I. C., and Arlett, C. F. (1997) *Free Radic. Biol. Med.* **22,** 343–347
26. Barlow, C., Dennery, P. A., Shigenaga, M. K., Smith, M. A., Morrow, J. D., Roberts, L. J., Wynshaw-Boris, A., and Levine, R. L. (1999) *Proc. Natl. Acad. Sci. U. S. A.* **96,** 9915–9919
27. Boyer, J. C., Kaufmann, W. K., Brylawski, B. P., and Cordeiro-Stone, M. (1990) *Cancer Res.* **50,** 2593–2598
28. Gilad, S., Barshira, A., Harnik, R., Shkedy, D., Ziv, Y., Khosravi, R., Brown, K., Vanagaite, L., Xu, G., Frydman, M., Lavin, M. F., Hill, D., Tagle, D. A., and Shiloh, Y. (1996) *Hum. Mol. Genet.* **5,** 2033–2037
29. Le, X. C., Xing, J. Z., Lee, J., Leadon, S. A., and Weinfeld, M. (1998) *Science* **280,** 1066–1069
30. Winston, G. W., Harvey, W., Berl, L., and Cederbaum, A. I. (1983) *Biochem. J.* **216,** 415–421
31. Vuillaume, M., Calvayrac, R., Best Belpomme, M., Tarroux, P., Hubert, M., Decroix, Y., and Sarasin, A. (1986) *Cancer Res.* **46,** 538–544
32. Watters, D., Kedar, P., Spring, K., Bjorkman, J., Chen, P., Gatei, M., Birrell, G., Garrone, B., Srinivasa, P., Crane, D. I., and Lavin, M. F. (1999) *J. Biol. Chem.* **274,** 34277–34282
33. Shackelford, R. E., Kaufmann, W. K., and Paules, R. S. (1999) *Environ. Health Perspect.* **107,** 5–24
34. Regoli, F., and Winston, G. W. (1999) *Toxicol. Appl. Pharmacol.* **156,** 96–105
35. Beamish, H., Khanna, K. K., and Lavin, M. F. (1994) *Radiat. Res.* **138,** 5130–5133
36. Kastan, M. B., Zhan, Q., El Deiry, W. S., Carrier, F., Jacks, T., Walsh, W. V., Plunkett, B. S., Vogelstein, B., and Fornace, A. J. (1992) *Cell* **71,** 587–597
37. Canman, C. E., Wolff, A. C., Chen, C. Y., Fornace, A. J., and Kastan, M. B. (1994) *Cancer Res.* **54,** 5054–5058
38. Xie, G. F., Habbersett, R. C., Jia, Y. W., Peterson, S. R., Lehnert, B. E., Bradbury, E. M., and Danna, J. A. (1998) *Oncogene* **16,** 721–736
39. Ohtsubo, M., Theodoras, A. M., Schumacher, J., Roberts, J. M., and Pagano, M. (1995) *Mol. Cell. Biol.* **15,** 2612–2624
40. Kaufmann, W. K., Schwartz, J. L., Hurt, J. C., Byrd, L. L., Galloway, D. A., Levedakou, E., and Paules, R. S. (1997) *Cell Growth Differ.* **8,** 1105–1114
41. Kaufmann, W. K., Levedakou, E. N., Grady, H. L., Paules, R. S., and Stein, G. H. (1995) *Cancer Res.* **55,** 7–11
42. Keyse, S. M., and Tyrrell, R. M. (1989) *Proc. Natl. Acad. Sci. U. S. A.* **86,** 99–103
43. Conger, A. D., and Fairchild, L. M. (1952) *Proc. Natl. Acad. Sci. U. S. A.* **38,** 289–299
44. Flattery-O'Brien, J. A., and Dawes, I. W. (1998) *J. Biol. Chem.* **273,** 8564–8571
45. Gowen, L. C., Avrutskaya, A. V., Latour, A. M., Koller, B. H., and Leadon, S. A. (1998) *Science* **281,** 1009–1012
46. Cortez, D., Wang, Y., Qin, J., and Elledge, S. J. (1999) *Science* **286,** 1162–1166
47. Sedgwick, R. P., and Boder, E. (1991) in *Handbook of Clinical Neurology* (Vinkins, P. J., Bruyn, G. W., and Klawans, H. L., eds) Vol. 6, pp. 347–423, John Wiley & Sons, New York
48. Boder, E., and Sedgwick, R. P. (1970) *Psychiatr. Neurol. Med. Psychol. Beih.* **13–14,** 8–16
49. Boder, E. (1985) *Kroc Found. Ser.* **19,** 1–63
50. El-Deiry, W. S., Harper, J. W., O'Connor, P. M., Velculescu, V. E., Canman, C. E., Jackman, J., Pietenpol, J. A., Burrell, M., Hill, D. E., Wang, Y., Wiman, K. G., Mercer, W. E., Kastan, M. B., Kohn, K. W., Elledge, S. J., Kinzler, K. W., and Vogelstein, B. (1994) *Cancer Res.* **54,** 1169–1174